MDPI

Article

Features of the Phase Preferences, Long- and Short-Range Order in $Ln_2(WO_4)_3$ (*Ln* = Gd, Dy, Ho, Yb) with Their Relation to Hydration Behavior

Victor V. Popov [1,2]*, Yan V. Zubavichus [3]*, Alexey P. Menushenkov[1], Alexey A. Yastrebtsev[1], Bulat R. Gaynanov[1], Sergey G. Rudakov[1], Andrey A. Ivanov[1], Fyodor E. Dubyago[1], Roman D. Svetogorov[2], Evgeny V. Khramov[2], Nadezhda A. Tsarenko[4], Nataliya V. Ognevskaya[4], Igor V. Shchetinin[5]

1 Department of Solid State Physics and Nanosystems, National Research Nuclear University MEPhI (Moscow Engineering Physics Institute), Moscow, 115409, Russia
2 Kurchatov Synchrotron Radiation Source, National Research Center Kurchatov Institute, Moscow, 123182, Russia
3 Synchrotron Radiation Facility SKIF, Boreskov Institute of Catalysis SB RAS, Koltsovo, 630559, Russia
4 JSC Design & Survey and Research & Development Institute of Industrial Technology, Moscow, 115409, Russia
5 Material Science Department, National University of Science and Technology MISiS, Moscow, 119049, Russia
* Correspondence: vvpopov@mephi.ru (V. V. P.); yvz@catalysis.ru (Y. V. Z.)

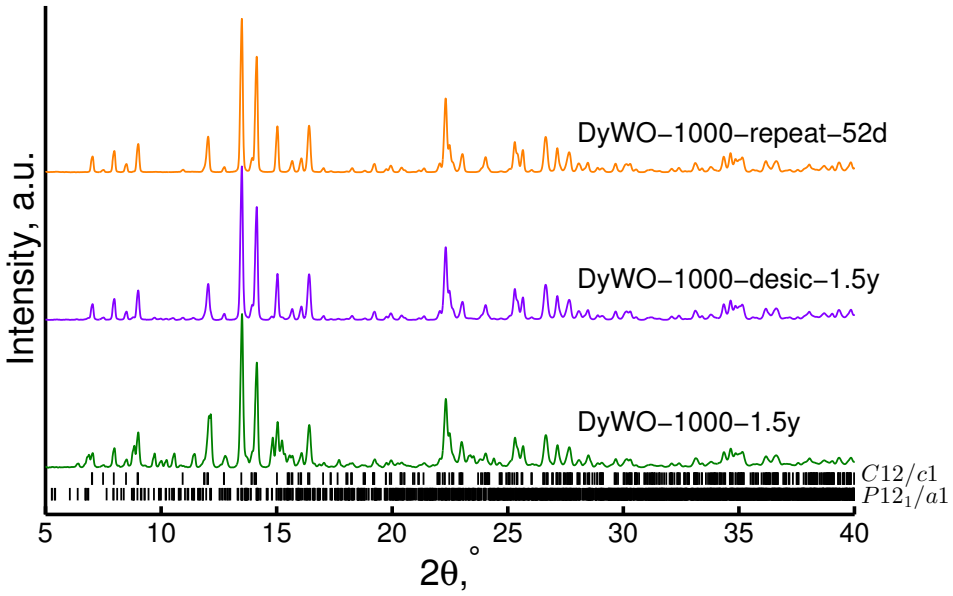

Figure S1. XRD patterns of $Dy_2(WO_4)_3$ powders prepared under different conditions. A detailed description of samples' codenames are given in Table 1 of the main text.

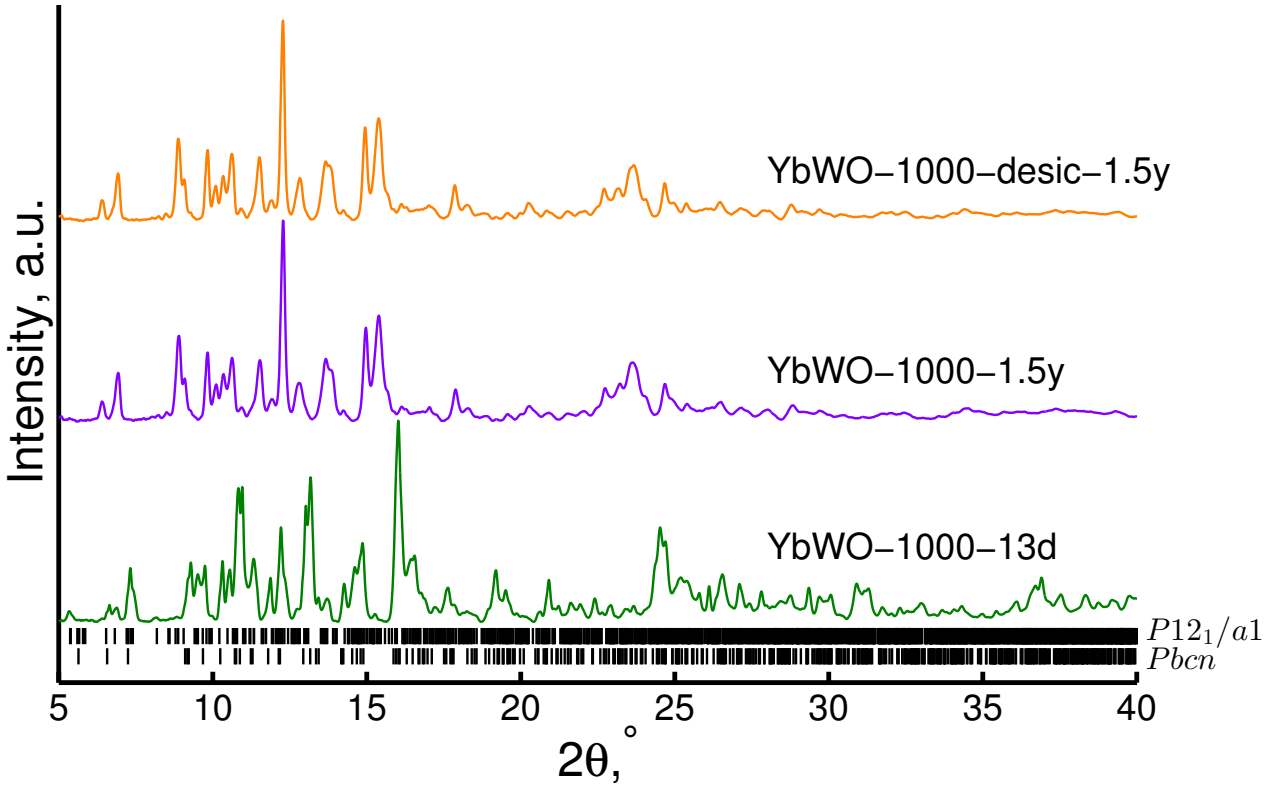

Figure S2. XRD patterns of $Yb_2(WO_4)_3$ powders prepared under different conditions. A detailed description of samples' codenames are given in Table 1 of the main text.

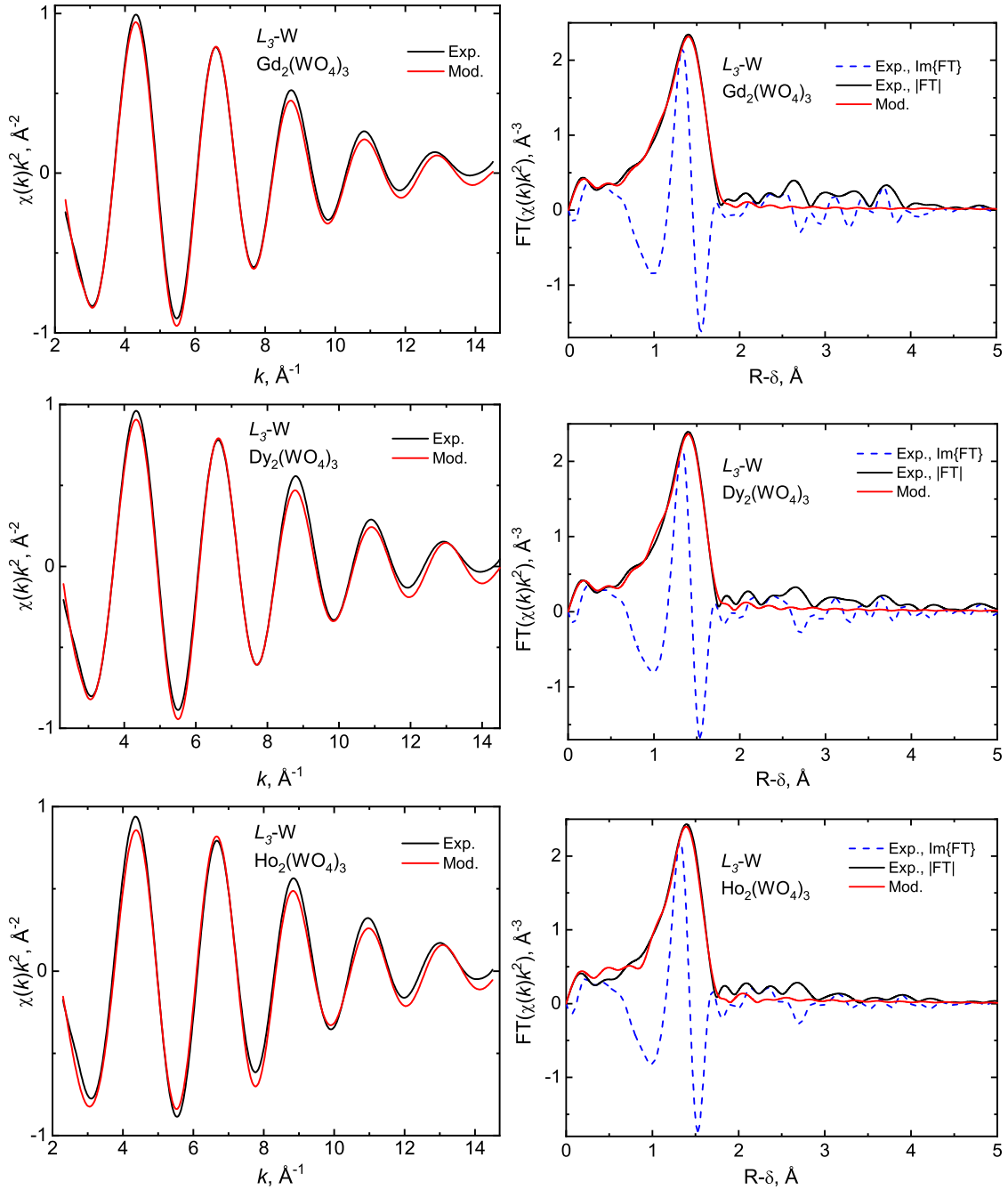

Figure S3. The experimental and fitted k^2-weighted EXAFS-functions $\chi(k)k^2$ (left panel) measured above the L_3-W edge and their Fourier transform magnitudes and imaginary parts (right panel) for the series of well-crystallized $Ln_2(WO_4)_3$-1000°C (*Ln* = Gd, Dy, Ho) powders. Best-fit curves correspond to the local-structure parameters given in Table 3 of the main text.

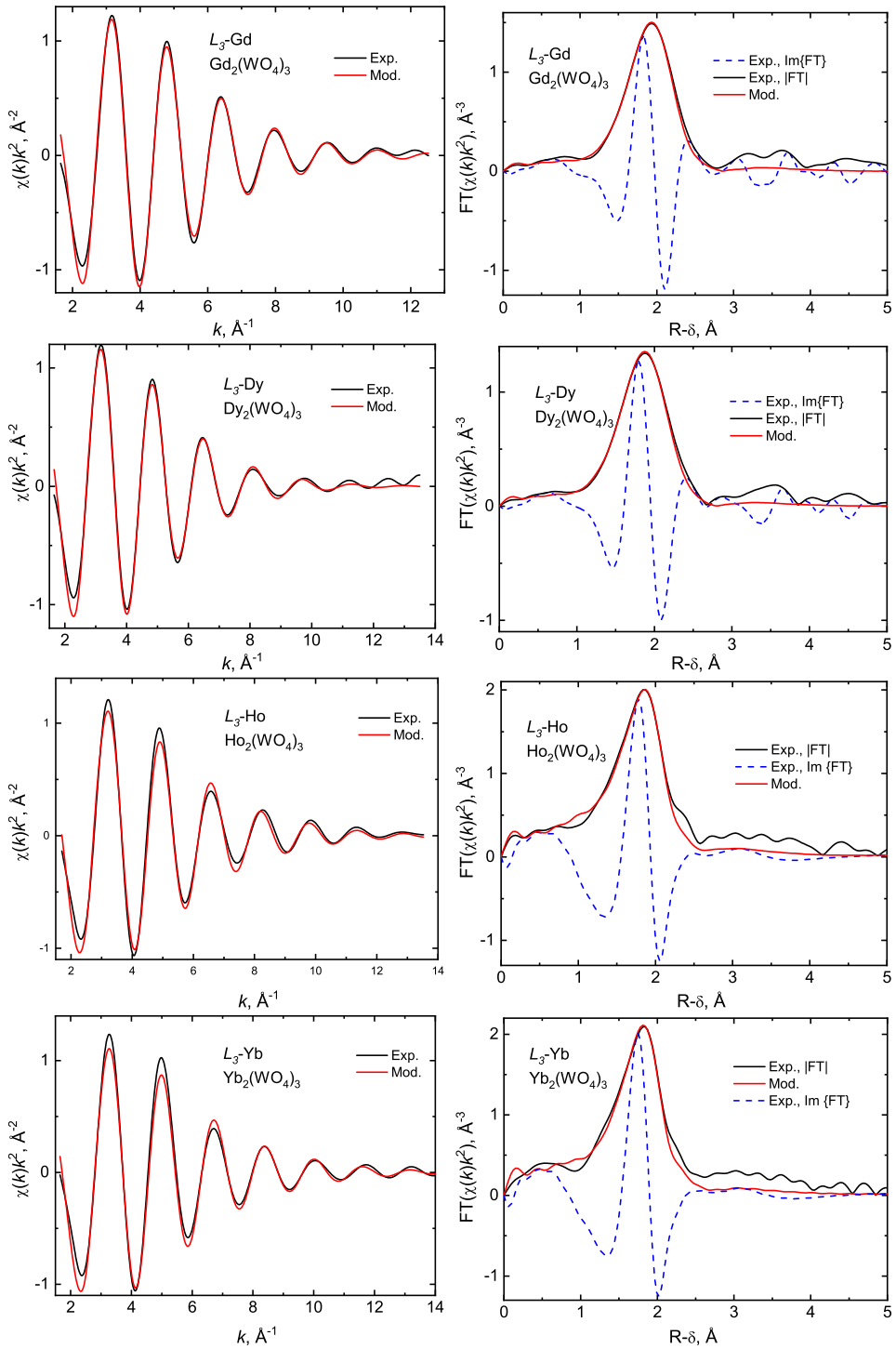

Figure S4. The experimental and fitted k^2-weighted EXAFS-functions $\chi(k)k^2$ (left panel) measured above the L_3-*Ln* edge and their Fourier transform magnitudes and imaginary parts (right panel) for the series of well-crystallized $Ln_2(WO_4)_3$-1000°C (*Ln* = Gd, Dy, Ho, Yb) powders. Best-fit curves correspond to the local-structure parameters given in Table 4 of the main text.

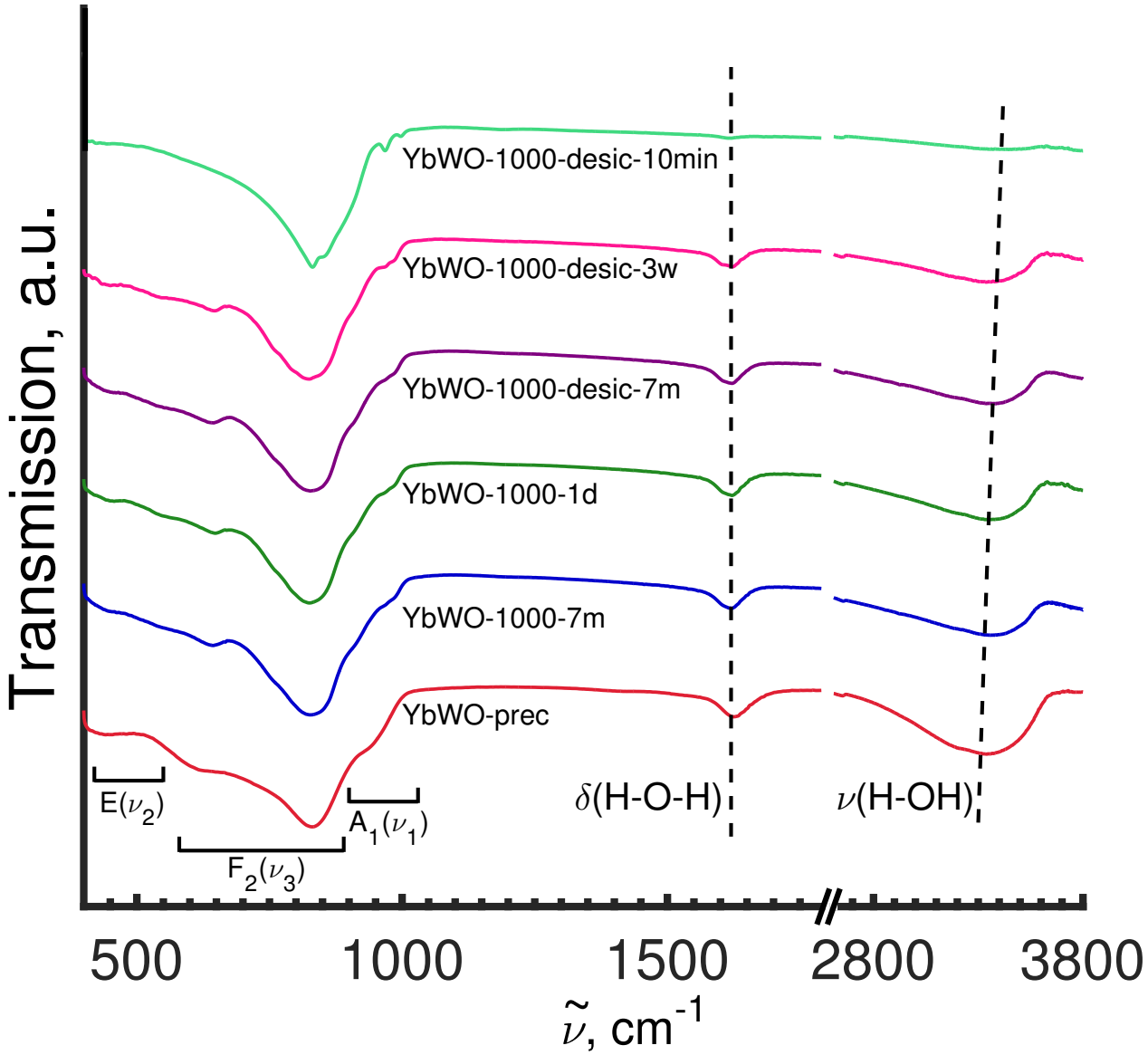

Figure S5. FT-IR spectra of $Yb_2(WO_4)_3$ powders prepared under different conditions.

Table S1. Composition, crystal structure and lattice parameters of heavy *Ln* tungstates according to literature

Composition	Type of crystal structure (sp. gr.)	Lattice parameters	References
$Y_2(WO_4)_3$	Orthorhombic	a = 10.0838 Å; b = 13.9593 Å; c = 9.9705 Å; V = 1386.2 Å^3	[1]
	Orthorhombic (sp. gr. *Pnca*)	a = 10.074(2) Å; b = 13.952(2) Å; c = 9.990(2) Å; V = 1404.4(3) Å^3	[2]
$Y_2(WO_4)_3 \cdot 3H_2O$	Structure B (tri-hydrate formed hygroscopically)	N/A	[3]
	Monoclinic (sp. gr. *P2/m*)	a = 14.308 Å; b = 4.354 Å; c = 12.430 Å; β = 119.78°; V = 672.1 Å^3	[4]
	Monoclinic	a = 16.3735 Å; b = 10.1174 Å; c = 19.3726 Å; β = 125.51°; V = 2954.99 Å^3	[1]
	Psuedo-orthorhombic	a = 10.1174 Å; b = 13.3301 Å; c = 9.6863 Å; β = 89.24°; V = 1287.74 Å^3	[1]
	Orthorhombic	a = 10.098(1) Å; b = 13.315(3) Å; c = 9.691(4) Å; V = 1303.1(4) Å^3	[2]
$Y_2(WO_4)_3 \cdot 2.5H_2O$	Monoclinic (sp. gr. *P2/m*)	a = 16.7267 Å; b = 10.0449 Å; c = 19.2045 Å; β = 126.91°; V = 2942.70 Å^3	[5]
$Dy_2(WO_4)_3$	Monoclinic (sp. gr. *C*12/*c*1)	a = 7.5981(1) Å; b = 11.3220(1) Å, c = 11.3254(1) Å; β = 109.8001(3)°; V = 962.76 Å^3	[6]
	Orthorhombic (sp. gr. *Pnca*)	a = 7.613(3) Å; b = 11.362(7) Å; c = 11.351(4) Å; V = 925.3(8) Å^3	[2]
$Ho_2(WO_4)_3$	Monoclinic	a = 7.5861(2) Å; b = 11.3157(3) Å, c = 11.3062(3) Å; β = 109.751(1)°; V = 913.45(5) Å^3 (unhydrated at 200°C)	[7]
$Ho_2(WO_4)_3 \cdot 3H_2O$	Structure B (tri-hydrate formed hygroscopically)	N/A	[3]
$Er_2(WO_4)_3$	Orthorhombic (sp. gr. *Pnca*)	a = 10.045(3) Å; b = 13.900(3) Å; c = 9.949(2) Å; V = 1389.4(4) Å^3	[2]
$Er_2(WO_4)_3 \cdot 3H_2O$	Orthorhombic	a = 10.083(5) Å; b = 13.246(6) Å; c = 9.675(5) Å; V = 1292.2(8) Å^3	[2]
$Tm_2(WO_4)_3$	Orthorhombic	a = 9.9809(8) Å; b = 13.8294(10) Å; c = 9.8953(8) Å; V = 1365.8(2) Å^3 (unhydrated at 200°C)	[7]
$Yb_2(WO_4)_3$	Orthorhombic (sp. gr. *Pnca*)	a = 9.970(5) Å; b = 13.810(6) Å; c = 9.887(4) Å; V = 1361.5(8) Å^3	[2]
$Yb_2(WO_4)_3 \cdot 3H_2O$	Orthorhombic	a = 10.046(4) Å; b = 13.164(4) Å; c = 9.598(4) Å; V = 1269.4(6) Å^3	[2]
$Lu_2(WO_4)_3$	Orthorhombic (sp. gr. *Pnca*)	a = 9.982(4) Å; b = 13.806(4) Å; c = 9.888(3) Å; V = 1362.6(6) Å^3	[2]
	Orthorhombic (sp. gr. *Pbcn*)	a = 13.782 Å; b = 9.873 Å; c = 9.961 Å; V = 1355.4 Å^3	[8]
$Lu_2(WO_4)_3 \cdot 3H_2O$	Orthorhombic	a = 10.050(5) Å; b = 13.179(8) Å; c = 9.584(6) Å; V = 1269.5(9) Å^3	[2]

N/A - not available

Table S2. The full list of sample codenames under study

#	Ln type	Sample codename	Technique(s) applied	Apparent hydration degree / Chemical composition	Phase Composition
1	Gd	GdWO-prec	STA, XRD, Raman, FT-IR	$Gd_2(WO_4)_3 \cdot 5.0H_2O$	Amorphous
2	Gd	GdWO-500-6d	XRD, Raman, FT-IR		Amorphous
3	Gd	GdWO-550-6d	XRD, Raman, FT-IR		Amorphous
4	Gd	GdWO-600-6d	XRD, Raman, FT-IR		$C12/c1$
5	Gd	GdWO-700-6d	XRD, Raman, FT-IR		$C12/c1$
6	Gd	GdWO-800-6d	XRD, Raman, FT-IR		$C12/c1$
7	Gd	GdWO-900-6d	XRD, Raman, FT-IR		$C12/c1$
8	Gd	GdWO-1000-14d	s-XRD		$C12/c1$
9	Gd	GdWO-1000-1.5y	STA, s-XRD, XANES/EXAFS, Raman, FT-IR	$Gd_2(WO_4)_3 \cdot 0.02H_2O$	$C12/c1$
10	Dy	DyWO-prec	STA, XRD, Raman, FT-IR	$Dy_2(WO_4)_3 \cdot 4.8H_2O$	Amorphous
11	Dy	DyWO-600-6d	XRD		$C12/c1$
12	Dy	DyWO-1000-1d	STA, FT-IR	$Dy_2(WO_4)_3 \cdot 1.7H_2O$	
13	Dy	DyWO-1000-9d	STA	$Dy_2(WO_4)_3 \cdot 1.8H_2O$	
14	Dy	DyWO-1000-11d	s-XRD		$0.57C12/c1 + 0.43\ P12_1/a1$
15	Dy	DyWO-1000-7m	FT-IR		
16	Dy	DyWO-1000-1.5y	STA, s-XRD, XANES/EXAFS, Raman	$Dy_2(WO_4)_3 \cdot 1.8H_2O$ or $0.47\ Dy_2(WO_4)_3(C12/c1) + 0.53\ Dy_2(WO_4)_3 \cdot 3.4H_2O\ (P12_1/a1)$	$0.47C12/c1 + 0.53P12_1/a1$
17	Dy	DyWO-1000-desic-10min	Raman, FT-IR		
18	Dy	DyWO-1000-desic-7m	FT-IR		
19	Dy	DyWO-1000-desic-1.5y	STA, s-XRD, Raman	$Dy_2(WO_4)_3 \cdot 0.5H_2O$	$0.88C12/c1 + 0.12P12_1/a1$
20	Dy	DyWO-1000-repeat-1d	FT-IR		
21	Dy	DyWO-1000-repeat-7d	STA	$Dy_2(WO_4)_3 \cdot 0.02H_2O$	
22	Dy	DyWO-1000-repeat-52d	s-XRD		$C12/c1$
23	Ho	HoWO-prec	STA, XRD, Raman, FT-IR	$Ho_2(WO_4)_3 \cdot 5.4H_2O$	Amorphous
24	Ho	HoWO-600-6d	XRD		Amorphous
25	Ho	HoWO-1000-1d	STA, FT-IR	$Ho_2(WO_4)_3 \cdot 3.1H_2O$	
26	Ho	HoWO-1000-7d	STA	$Ho_2(WO_4)_3 \cdot 3.3H_2O$	
27	Ho	HoWO-1000-9d	s-XRD		$P12_1/a1$
28	Ho	HoWO-1000-7m	FT-IR		
29	Ho	HoWO-1000-1.5y	STA, s-XRD, XANES/EXAFS, Raman	$Ho_2(WO_4)_3 \cdot 3.5H_2O$	$P12_1/a1$
30	Ho	HoWO-1000-desic-10min	Raman, FT-IR		
31	Ho	HoWO-1000-desic-3w	FT-IR		
32	Ho	HoWO-1000-desic-7m	FT-IR		
33	Ho	HoWO-1000-desic-1.5y	STA, s-XRD, Raman	$Ho_2(WO_4)_3 \cdot 3.3H_2O$	$P12_1/a1$

34	Ho	HoWO-1000-repeat-7d	STA	$Ho_2(WO_4)_3{\cdot}3.0H_2O$	
35	Yb	YbWO-prec	STA, XRD, Raman, FT-IR	$Yb_2(WO_4)_3{\cdot}4.7H_2O$	Amorphous
36	Yb	YbWO-600-6d	XRD		$P12_1/a1$
37	Yb	YbWO-1000-1d	STA, FT-IR	$Yb_2(WO_4)_3{\cdot}3.0H_2O$	
38	Yb	YbWO-1000-9d	STA	$Yb_2(WO_4)_3{\cdot}3.1H_2O$	
39	Yb	YbWO-1000-13d	s-XRD		$0.5P12_1/a1 + 0.5Pbcn$
40	Yb	YbWO-1000-7m	FT-IR		
41	Yb	YbWO-1000-1.5y	STA, s-XRD, XANES/EXAFS, Raman	$Yb_2(WO_4)_3{\cdot}3.1H_2O$	$P12_1/a1$
42	Yb	YbWO-1000-desic-10min	Raman, FT-IR		
43	Yb	YbWO-1000-desic-3w	FT-IR		
44	Yb	YbWO-1000-desic-7m	FT-IR		
45	Yb	YbWO-1000-desic-1.5y	STA, s-XRD, Raman	$Yb_2(WO_4)_3{\cdot}3.1H_2O$	$P12_1/a1$
46	Yb	YbWO-1000-repeat-9d	STA	$Yb_2(WO_4)_3{\cdot}3.1H_2O$	

Table S3. STA results of well-crystallized *Ln*WO-1000 (*Ln*=Gd, Dy, Ho, Yb) powders stored in air for different periods of time

Sample	Dehydration (at 200°C)			
	$T_{deh.}$, ° C	$\Delta H_{deh.}$, J/g	Δm, %	nH_2O
GdWO-1000-1.5y	-	-	0.03	0.02
DyWO-1000-1d	91.0 (shoulder) 109.7	111	2.7	1.7
DyWO-1000-9d	109.3	112	2.9	1.8
DyWO-1000-1.5y	127.9	110	2.9	1.8 (3.4*)
DyWO-1000-desic-1.5y	113.1	30.4	0.8	0.5
DyWO-1000-repeat-7d	-	-	0.03	0.02
HoWO-1000-1d	86.4 (shoulder) 106.4	208	5.0	3.1
HoWO-1000-7d	107.7	209	5.3	3.3
HoWO-1000-1.5y	117.9	229	5.5	3.5
HoWO-1000-desic-1.5y	109.1	217	5.2	3.3
HoWO-1000-repeat-7d	106.6	199	4.8	3.0
YbWO-1000-1d	76.8	185	4.7	3.0
YbWO-1000-9d	86.1	198	5.0	3.1
YbWO-1000-1.5y	98.9	199	5.0	3.1
YbWO-1000-desic-1.5y	94	188	5.0	3.1
YbWO-1000-repeat-9d	92.6	200	5.0	3.1

*Recalculated taking into account the volume fraction of the $P12_1/a1$ phase (see Table S4)

Table S4. Rietveld refinement of s-XRD patterns for well-crystallized powders of $Ln_2(WO_4)_3$-1000° C (*Ln* = Gd, Dy, Ho, Yb)

Sample	Structure (space group)	Content, %	Cell param., a, b, c, Å, β,°	Cell vol., Å^3	^aL, nm	$^b\epsilon$, %	R_p,%/ R_{wp},%	$^cS_{GoF}$
GdWO-1000-14d	Monoclinic (*C*12/*c*1 (15))	100	a = 7.6593(4) b = 11.4299(6) c = 11.4093(6) β = 109.752(2)	940.07(8)	286(15)	0.192(9)	6.20/ 8.52	1.36
GdWO-1000-1.5y	Monoclinic (C12/*c*1 (15))	100	a = 7.6581(6) b = 11.4282(9) c = 11.4071(10) β = 109.764(3)	939.52(13)	104(3)	0.050(15)	7.64/ 11.43	1.26
DyWO-1000-11d	Monoclinic (C12/*c*1 (15))	56.7(3)	a = 7.6001(2) b = 11.3335(2) c = 11.3434(3) β = 109.785(2)	919.39(3)	171(5)	0.417(9)	7.45/ 11.92	1.64
	Monoclinic ($P12_1/a1$ (14))	43.3(3)	a = 16.645(2) b = 10.1359(7) c = 19.407(2) β = 126.268(5)	2639.9(4)	187(27)	0.554(49)		
DyWO-1000-1.5y	Monoclinic (C12/*c*1 (15))	47.3(3)	a = 7.5966(2) b = 11.3295(3) c = 11.3394(4) β = 109.784(3)	918.33(5)	99(3)	0.358(15)	8.01/ 11.85	1.17
	Monoclinic ($P12_1/a1$ (14))	52.7(3)	a = 16.423(2) b = 10.1219(7) c = 19.438(2) β = 126.061(8)	2612.1(5)	78(5)	0.287(48)		
DyWO-1000-desic-1.5y	Monoclinic (C12/*c*1 (15))	88.2(5)	a = 7.5984(2) b = 11.3302(2) c = 11.3387(3) β = 109.788(2)	918.52(4)	152(5)	0.359(10)	8.56/ 12.30	1.39
	Monoclinic ($P12_1/a1$ (14))	11.8(5)	a = 16.677(12) b = 10.115(5) c = 19.494(11) β = 126.56(4)	2641.0(9)	84(13)	0.359(10)		
DyWO-1000-repeat-52d	Monoclinic (C12/*c*1 (15))	100	a = 7.5987(7) b = 11.3335(10) c = 11.3400(10) β = 109.788(3)	918.93(14)	137(6)	0.208(16)	10.70/ 14.94	2.09
HoWO-1000-9d	Monoclinic ($P12_1/a1$ (14))	100	a = 16.591(2) b = 10.1091(6) c = 19.351(2) β = 126.356(3)	2613.8(3)	485(95)	1.020(26)	9.04/ 13.42	1.72
HoWO-1000-1.5y	Monoclinic ($P12_1/a1$ (14))	100	a = 16.362(2) b = 10.0980(6) c = 19.376(2) β = 126.062(5)	2587.9(4)	100(5)	0.589(30)	10.79/ 14.89	1.36
HoWO-1000-desic-1.5y	Monoclinic ($P12_1/a1$ (14))	100	a = 16.565(2) b = 10.1094(6) c = 19.345(2) β = 126.366(3)	2608.6(3)	223(21)	0.902(27)	9.38/ 12.92	1.14
YbWO-1000-13d	Monoclinic	49.6(4)	a = 16.517(2)	2565.3(6)	76(3)	0.927(26)	7.72 /	1.40

	($P12_1/a1$ (14))		b = 10.0274(12) c = 19.221(2) β = 126.312(7)				12.16	
	Orthorhombic ($Pbcn$ (60))	50.4(4)	a = 13.8085(6) b = 9.8956(5) c = 9.9721(5)	1362.62(12)	77(3)	0.377(23)		
YbWO-1000-1.5y	Monoclinic ($P12_1/a1$ (14))	100	a = 16.461(2) b = 10.0022(9) c = 19.215(2) β = 126.335(4)	2548.5(5)	256(39)	1.478(39)	8.72/ 12.27	1.04
YbWO-1000-desic-1.5y	Monoclinic ($P12_1/a1$ (14))	100	a = 16.453(2) b = 10.0195(7) c = 19.205(2) β = 126.333(3)	2550.4(4)	206(20)	1.213(30)	7.33/ 10.49	1.03

[a] L - the crystallite size; [b] ϵ - the microstrain value; [c] S_{GoF} - the goodness-of-fit.

Table S5. Atomic coordinates for the HoWO-1000-1.5y sample according to the Rietveld refinement. The nominal chemical composition of the phase is $Ho_2(WO_4)_3 \cdot 3H_2O$

Atom*	x	y	z	Uiso
Ho1	0.5949	0.5152	0.4248	0.0137
Ho2	0.3528	0.49	0.0427	0.0137
Ho3	-0.1305	0.5154	-0.1936	0.0137
Ho4	-0.3703	0.0041	-0.3222	0.0137
W1	0.5163	0.261	0.4957	0.064
W2	0.5921	0.4001	0.2329	0.064
W3	0.1088	0.6603	-0.1531	0.064
W4	0.0242	0.7523	0.0115	0.064
W5	-0.315	0.3124	-0.1893	0.064
W6	-0.6378	0.1306	-0.3927	0.064
O1	0.4725	0.1127	0.4529	0.1
O2	0.4383	0.3557	0.5015	0.1
O3	0.5945	0.1889	0.5939	0.1
O4	0.5482	0.3536	0.4437	0.1
O5	0.7692	0.4583	0.5305	0.1
O6	0.4319	0.5661	0.3116	0.1
O7	0.6568	0.6938	0.3913	0.1
O8	0.6164	0.3935	0.3324	0.1
O9	0.6515	0.2526	0.2512	0.1
O10	0.6878	0.5024	0.2623	0.1
O11	0.5135	0.4351	0.1309	0.1
O12	0.4443	0.6423	0.0131	0.1
O13	0.4015	0.2769	0.0165	0.1
O14	0.3348	0.3015	0.0992	0.1
O15	0.327	0.6334	0.1136	0.1
O16	0.1968	0.5396	-0.1081	0.1
O17	0.0806	0.7205	-0.2465	0.1
O18	0.0066	0.5841	-0.1729	0.1
O19	-0.1509	0.4331	-0.324	0.1
O20	-0.0344	0.3101	-0.0925	0.1
O21	-0.0508	0.6313	-0.0533	0.1
O22	-0.2542	0.4388	-0.1962	0.1
O23	-0.3438	0.1829	-0.2257	0.1
O24	-0.5327	0.0568	-0.3626	0.1
O1w	0.0785	0.7833	0.2329	0.1
O2w	0.3092	0.1337	0.4336	0.1
O3w	0.6717	0.2042	0.4391	0.1
O4w	0.8416	0.1711	0.3281	0.1
O5w	0.1452	0.8787	0.1254	0.1
O6w	0.2831	0.6958	-0.1633	0.1

*Atomic coordinates and thermal parameters of the oxygen atoms were refined with geometrical constraints. The thermal parameters of heavy atoms, i.e., Ho and W were refined but kept equal for identical elements. The thermal parameters of the oxygen atoms were not refined. Hydrogen atoms of water molecules were not located due to weak contribution to total scattering.

References

1. Sleight, A.W. Negative Thermal Expansion. *MRS Proc.* **2002**, *755*, 106.https://doi.org/10.1557/PROC-755-DD10.6.
2. Sumithra, S.; Umarji, A.M. Role of crystal structure on the thermal expansion of $Ln_2W_3O_{12}$ (*Ln* = La, Nd, Dy, Y, Er and Yb). *Solid State Sci.* **2004**, *6*, 1313–1319. https://doi.org/10.1016/j.solidstatesciences.2004.07.023.
3. Nassau, K.; Levinstein, H.J.; Loiacono, G.M. A comprehensive study of trivalent tungstates and molybdates of the type $L_2(MO_4)_3$. *J. Phys. Chem. Solids* **1965**, *26*, 1805–1816. https://doi.org/10.1016/0022-3697(65)90213-1.
4. Kol'tsova, T.N. X-ray diffraction study of $Y_2W_3O_{12}{\cdot}3H_2O$. *Inorg. Mater.* **2001**, *37*, 1175–1177.
5. Pontón, P.I.; Prisco, L.P.; Dosen, A.; Faro, G.S.; de Abreu, M.A.; Marinkovic, B.A. Co-precipitation synthesis of $Y_2W_3O_{12}$ submicronic powder. *Ceram. Int.* **2017**, *43*, 4222–4228. https://doi.org/10.1016/j.ceramint.2016.12.055.
6. Shen, R.; Wang, C.; Wang, T.; Dong, C.; Chen, X.; Liang, J. Crystal Structures of $Dy_2(WO_4)_3$ and $GdY(WO_4)_3$. *Rare Met.* **2003**, *22*, 49–54.
7. Xiao, X.; Cheng, Y.; Peng, J.; Wu, M.; Chen, D.; Hu, Z.; Kiyanagi, R.; Fieramosca, J.; Short, S.; Jorgensen, J. Thermal expansion properties of $A_2(MO_4)_3$ (A=Ho and Tm; M=W and Mo). *Solid State Sci.* **2008**, *10*, 321–325.
8. Shmurak, S.Z.; Kedrov, V.V.; Kiselev, A.P.; Fursova, T.N.; Zver'kova, I.I.; Khasanov, S.S. Spectral and Structural Characteristics of $(Lu_{1-x}Eu_x)_2(WO_4)_3$ Tungstates. *Phys. Solid State* **2019**, *61*, 2117–2129. https://doi.org/10.1134/S1063783419110325.